

Ste6p Mutants Defective in Exit from the Endoplasmic Reticulum (ER) Reveal Aspects of an ER Quality Control Pathway in *Saccharomyces cerevisiae*

Diego Loayza,* Amy Tam, Walter K. Schmidt, and Susan Michaelis[†]

Department of Cell Biology and Anatomy, The Johns Hopkins University School of Medicine, Baltimore, Maryland 21205

Submitted March 18, 1998; Accepted July 24, 1998

Monitoring Editor: Peter Walter

We are studying the intracellular trafficking of the multispanning membrane protein Ste6p, the a-factor transporter in *Saccharomyces cerevisiae* and a member of the ATP-binding cassette superfamily of proteins. In the present study, we have used Ste6p as model for studying the process of endoplasmic reticulum (ER) quality control, about which relatively little is known in yeast. We have identified three mutant forms of Ste6p that are aberrantly ER retained, as determined by immunofluorescence and subcellular fractionation. By pulse-chase metabolic labeling, we demonstrate that these mutants define two distinct classes. The single member of Class I, Ste6-166p, is highly unstable. We show that its degradation involves the ubiquitin-proteasome system, as indicated by its *in vivo* stabilization in certain ubiquitin-proteasome mutants or when cells are treated with the proteasome inhibitor drug MG132. The two Class II mutant proteins, Ste6-13p and Ste6-90p, are hyperstable relative to wild-type Ste6p and accumulate in the ER membrane. This represents the first report of a single protein in yeast for which distinct mutant forms can be channeled to different outcomes by the ER quality control system. We propose that these two classes of ER-retained Ste6p mutants may define distinct checkpoint steps in a linear pathway of ER quality control in yeast. In addition, a screen for high-copy suppressors of the mating defect of one of the ER-retained *ste6* mutants has identified a proteasome subunit, Hrd2p/p97, previously implicated in the regulated degradation of wild-type hydroxymethylglutaryl-CoA reductase in the ER membrane.

INTRODUCTION

Eukaryotic membrane and soluble proteins that are destined for transit through the secretory pathway are subject to a surveillance system known as "ER quality control" that retains aberrant proteins in the endoplasmic reticulum (ER) (Bonifacino and Lippincott-Schwartz, 1991; Hammond and Helenius, 1995). ER quality control ensures that only newly synthesized polypeptides that are correctly folded or assembled may exit the ER and proceed to their final destination. Misfolded or unassembled proteins that are ER-retained have been shown, in some cases, to be tran-

siently bound to chaperones and can subsequently be degraded by an ER-associated degradation (ERAD) mechanism, which involves the ubiquitin-proteasome system (Brodsky and McCracken, 1997; Kopito, 1997). Examples of misfolded mammalian proteins that are substrates for ER quality control and ERAD include mutant forms of CFTR, $\alpha 1$ antitrypsin, and the low-density lipoprotein receptor, which are associated with the diseases cystic fibrosis, emphysema, and familial hypercholesterolemia, respectively (Amara *et al.*, 1992; Thomas *et al.*, 1995; Ward *et al.*, 1995). The fate of ER-retained proteins varies; not all retained proteins are rapidly degraded. For instance, a temperature-sensitive mutant viral protein, VSV G ts045, is retained in the ER at nonpermissive temperature but is metabolically stable (Doms *et al.*, 1987). Upon a shift-down to permissive temperature, which presumably

* Present address: Department of Cell Biology and Genetics, Rockefeller University, New York, NY 10021.

[†] Corresponding author.

favors its proper folding, VSV G tsO45 is able to exit the ER. The factors that determine the precise fate (degradation vs. stabilization) of an ER-retained protein are not presently known.

An understanding of the cellular components that recognize misfolded proteins is lacking. Transmembrane proteins are of particular interest in this regard due to their multicompartamental topology. Mutations that affect either the cytosolic, transmembrane, or luminal domains of a polytopic membrane protein can cause misfolding and thereby recruit the ER quality control system (Kopito, 1997). One of the best characterized examples of a membrane protein whose trafficking is monitored and impeded by the ER quality control system is the mutant protein, CFTR Δ F508. The Δ F508 mutation, which results in the disease cystic fibrosis, generates a temperature-sensitive folding defect that leads to prolonged association of the mutant CFTR with the ER chaperone calnexin (Pind *et al.*, 1994). Calnexin may prevent the premature exit of mutant CFTR from the ER, perhaps by attempting to fold the protein. It is notable that calnexin, whose functional domain resides in the ER lumen, can detect the misfolding of CFTR Δ F508, since the Δ F508 mutation alters the nucleotide binding domain (NBD) of CFTR, a region predicted to be cytosolically oriented. Ultimately, the ER-retained CFTR Δ F508 is ubiquitinated and degraded by the 26S proteasome (Jensen *et al.*, 1995; Ward *et al.*, 1995). Elucidation of the fate of nascent CFTR Δ F508 has provided a framework for understanding the steps of quality control in mammalian cells, namely ER retention, chaperone binding, ubiquitination, and degradation via the proteasome. For certain proteins an additional step of "reverse translocation" from the ER to the cytosol may precede degradation by the proteasome, as recently suggested by studies of the major histocompatibility complex (MHC) class I protein (Wiertz *et al.*, 1996; Hughes *et al.*, 1997).

A growing body of evidence indicates that an ER quality control system exists in *Saccharomyces cerevisiae*. Mutant forms of the soluble proteins pro- α -factor (McCracken and Brodsky, 1996) and CPY (CPY*) (Hiller *et al.*, 1996) and the membrane protein Sec61-2p (Sommer and Jentsch, 1993) are ER-retained and subsequently degraded in a proteasome-dependent manner. For mutant α -factor and CPY*, like the mammalian MHC Class I protein, reverse translocation from the ER lumen into the cytosol appears to be a prerequisite for degradation (Pilon *et al.*, 1997; Plemper *et al.*, 1997). A yeast cell-free system has been developed recently that recapitulates the phenomenon of ERAD in vitro and can be used to biochemically identify the cellular components involved in this process (McCracken and Brodsky, 1996; Werner *et al.*, 1996). Both in vivo and in vitro studies are beginning to reveal new

mechanisms associated with ER quality control and ERAD in yeast.

Because of the tractability of yeast to genetic and biochemical dissection, we decided to use Ste6p, the α -factor transporter in yeast, as a model protein for defining the events involved in the processes of ER quality control and ERAD. Ste6p is a member of the ATP-binding cassette (ABC) superfamily of transporters (Berkower and Michaelis, 1996). Examples of eukaryotic ABC proteins include CFTR, the multidrug resistance protein encoded by MDR (P-glycoprotein), the multidrug-resistance-associated protein MRP, the sulfonyl urea receptor SUR, and other transporters involved in human disease (Taglicht and Michaelis, 1998). Most ABC proteins are composed of two homologous halves, each of which contains six transmembrane domains and an NBD. The major portions of Ste6p and other ABC transporters, in particular their NBDs, are predicted to be cytosolically disposed (Kuchler *et al.*, 1989; Geller *et al.*, 1996). Studies from this laboratory and others have shown that Ste6p exhibits a complex intracellular trafficking pattern (Berkower *et al.*, 1994; Kölling and Hollenberg, 1994). After its transit via the secretory pathway to the plasma membrane, Ste6p undergoes rapid and constitutive endocytosis, followed by delivery to the vacuole where it is degraded. Ubiquitination is necessary for the endocytosis of Ste6p (Kölling and Losko, 1997) and, surprisingly, both the vacuolar proteases and the proteasome influence its degradation in the vacuole (Loayza and Michaelis, 1998). The metabolic half-life of Ste6p is \sim 20 min. Despite its presumed site of function at the plasma membrane, Ste6p does not accumulate there due to its constitutive endocytosis (Berkower *et al.*, 1994; Kölling and Hollenberg, 1994).

In the present study, we sought to isolate mutant forms of Ste6p that are defective in exit from the ER. Such mutants are expected to allow genetic dissection of the ER quality control pathway in yeast. We identified two distinct classes of ER-retained *ste6* mutants. The Class I mutant, Ste6-166p, contains a C-terminal truncation and is ER-retained but rapidly degraded. We provide evidence that the degradation of this mutant protein involves the ubiquitin-proteasome machinery, as is the case for the mutant form of CFTR discussed above. In contrast, Class II mutants, represented by two alleles, Ste6-13p and Ste6-90p, aberrantly accumulate in the ER but show little degradation over time. We speculate that the two possible outcomes represented by these two classes of *ste6* mutants define two distinct steps in a linear pathway of ER quality control in yeast. In this study, we also report the isolation of the *HRD2* gene, which encodes a subunit of the 19S proteasome cap (Tsurumi *et al.*, 1996), as an allele-specific multicopy suppressor of the

Table 1. Yeast strains used in this study

Strain name	Genotype	Reference/source
BKY 36-3-6b-T1	<i>MATa his4-15 leu2-3,112 ura3-52 erg6Δ::LEU2</i>	Gaber <i>et al.</i> , 1989
MHY500	<i>MATa his3 leu2 ura3 lys2 trp1</i>	Chen <i>et al.</i> , 1993
MHY552	<i>MATa ubc6::HIS3 ubc7::LEU2 his3 leu2 ura3 lys2 trp1</i>	Chen <i>et al.</i> , 1993
MHY623	<i>MATa doa4::LEU2 his3 leu2 ura3 lys2 trp1</i>	Papa and Hochstrasser, 1993
MS10	<i>MATa ura3-52 leu2-3,112 ade2-101</i>	M. Rose
MS1907	<i>MATa pep4::LEU2 ade2-101 leu2-3,112 ura3-52</i>	M. Rose
NY431	<i>MATa ura3-52 sec18-1</i>	P. Novick
SM1058	<i>MATa ura3 leu2 trp1 his4 (EG123)</i>	Michaelis and Herskowitz, 1988
SM1068	<i>MATα lys1</i>	Michaelis and Herskowitz, 1988
SM1563	<i>MATa ste6Δ1::LEU2 ura3 leu2 trp1 his4</i>	Berkower <i>et al.</i> , 1994
SM1646	<i>MATa ste6Δ2::URA3 ura3 leu2 trp1 his4</i>	Berkower and Michaelis, 1991
SM2544	<i>MATa ura3 leu2 trp1 his4 ste6Δ4</i>	Loayza and Michaelis, 1998
SM2567	Transformant of SM2544 and pSM192	This study
SM2569	Transformant of SM2544 with pSM693	This study
SM2655	As MHY552 but switched to <i>MATa</i>	This study
SM2694	As MHY623 but switched to <i>MATa</i>	This study
SM2729	As SM1058 with <i>ste6-90::HAc</i> integrated at <i>STE6</i> locus	This study
SM2731	Transformant of MHY500 with pSM1082	This study
SM2733	Transformant of MHY500 with pSM693	This study
SM2734	Transformant of SM2694 with pSM1083	This study
SM2735	Transformant of SM2694 with pSM1082	This study
SM2782	As SM1058 with <i>ste6-13::HAc</i> integrated at <i>STE6</i> locus	This study
SM2807	Transformant of NY431 with pSM1083	This study
SM2914	Transformant of SM2544 with pSM672	This study
SM2915	Transformant of SM2544 with pSM1085	Romano <i>et al.</i> , 1998
SM2916	Transformant of SM2544 with pSM1144	This study
SM2917	Transformant of SM2544 with pSM1084	This study
SM2918	Transformant of SM2544 with pSM1086	This study
SM2919	Transformant of SM2544 with pSM1087	This study
SM3032	Transformant of SM2655 with pSM1082	This study
SM3045	Transformant of SM2544 with pSM1126	This study
SM3154	Transformant of SM2544 with pSM1080	This study
SM3156	Transformant of SM2544 with pSM1081	This study
SM3289	Transformant of WCG4a with pSM1083	This study
SM3291	Transformant of WCG4/11/21a with pSM1083	This study
SM3460	Transformant of SM2729 with pSM217	This study
SM3461	Transformant of SM2782 with pSM217	This study
SM3479	Transformant of SM2729 with pSM1267	This study
SM3486	Transformant of SM2544 with pSM1126 and pSM1267	This study
SM3488	Transformant of SM2544 with pSM217 and pSM1126	This study
SM3548	Transformant of SM2544 with pSM672 and YEp105	This study
SM3550	Transformant of SM2544 with pSM1082 and YEp105	This study
SM3599	Transformant of BKY 36-3-6b-T1 with pSM1083	This study
SM3627	Transformant of MHY500 with pSM1083	This study
SM3661	Transformant of SM2544 with pSM1082	This study
SM3662	Transformant of NY431 with pSM683	This study
SM3663	Transformant of MS10 with pSM683	This study
SM3664	Transformant of MS10 with pSM1083	This study
SM3665	Transformant of MS1907 with pSM683	This study
SM3666	Transformant of MS1907 with pSM1083	This study
SM3667	Transformant of SM2655 with pSM1083	This study
SM3668	Transformant of SM2544 with pSM1086 and YEp105	This study
SM3669	Transformant of SM1646 with pSM435 and YEp105	This study
SM3884	Transformant of SM2782 with pSM1267	This study
WCG4a	<i>MATa ura3 leu2-3,112 his3-11,15</i>	Heinemeyer <i>et al.</i> , 1991
WCG4-11/21a	As WCG4a but <i>pre1-1 pre2-1</i>	Heinemeyer <i>et al.</i> , 1991

mating defect associated with two of the *ste6* alleles described in this study. Hrd2p is also known to play a role in the regulated degradation of the hydroxymethylglutaryl (HMG)-CoA reductase in the ER membrane

(Hampton *et al.*, 1996). An interesting possibility is that the 26S proteasome may be involved in the decision to retain misfolded or even normal proteins, in addition to participating in their degradation.

Table 2. Plasmids used in this study

Plasmid	Genotype	Reference
pRS316	<i>CEN URA3</i>	Sikorski and Hieter, 1989
pSM192	<i>CEN URA3 STE6</i>	Berkower and Michaelis, 1991
pSM217	<i>2μ URA3</i>	Berkower and Michaelis, 1991
pSM435	<i>2μ LEU2 STE6</i>	Berkower and Michaelis, 1991
pSM500	<i>2μ LEU2 STE6::HAc</i>	Paddon <i>et al.</i> , 1996
pSM683	<i>CEN URA3 STE6::HAe</i>	Loayza and Michaelis, 1998
pSM672	<i>2μ URA3 STE6::HAc</i>	Berkower, 1995
pSM693	<i>2μ URA3 STE6::HAe</i>	Berkower <i>et al.</i> , 1994
pSM954	<i>Ylp URA3 ste6-13::HAc</i>	This study
pSM955	<i>Ylp URA3 ste6-90::HAc</i>	This study
pSM1080	<i>2μ URA3 ste6-90,166::HAc</i>	This study
pSM1081	<i>2μ URA3 ste6-166::HAe</i>	This study
pSM1082	<i>2μ URA3 ste6-166::HAe</i>	This study
pSM1083	<i>CEN URA3 ste6-166::HAe</i>	This study
pSM1084	<i>CEN URA3 ste6-90::HAc</i>	This study
pSM1085	<i>CEN URA3 STE6::HAc</i>	Romano <i>et al.</i> , 1998
pSM1086	<i>2μ URA3 ste6-13::HAc</i>	This study
pSM1087	<i>2μ URA3 ste6-90::HAc</i>	This study
pSM1126	<i>CEN LEU2 ste6-166::HAe</i>	This study
pSM1144	<i>CEN URA3 ste6-13::HA</i>	This study
pSM1267	<i>2μ URA3 containing HRD2 locus (from YEp24 library)</i>	This study
pSM1347	<i>As pSM1267, with HRD2 gene inactivated at SacII site</i>	This study
YEp105	<i>2μ TRP1 ubi::myc</i>	Hochstrasser <i>et al.</i> , 1991

MATERIALS AND METHODS

Strains, Media, and Growth Conditions

Yeast strains used in this study are listed in Table 1. The strain SM2729, which bears the *ste6-90* mutation at the chromosomal *STE6* locus, was created by the two-step gene replacement method. First, *Sna*BI-linearized pSM955 (see below) was transformed into SM1058, and *Ura*⁺ transformants were selected. Second, segregants that had recombined out the plasmid were selected on 5-FOA. These were screened first for a mating defect to identify candidates with the *ste6-90* mutation and second by Western analysis for those with the triply iterated hemagglutinin epitope (HA) tag integrated in the genome. The gene replacement was confirmed by Southern blot. The strain SM2782, which contains the *ste6-13* mutation at the *STE6* locus, was constructed using an identical strategy, starting with pSM954 linearized with *Sna*BI. Plate and liquid dropout media were prepared as previously described (Michaelis and Herskowitz, 1988; Kaiser *et al.*, 1994). All yeast transformants were obtained by standard plasmid transformation techniques (Ito *et al.*, 1983; Elble, 1992). Cultures were grown at 30°C except where indicated.

Plasmid Constructions

Plasmids used in this study are listed in Table 2. Vectors were described by Sikorski and Hieter (1989). To detect Ste6p by immunofluorescence, immunoprecipitation, or immunoblotting, we used plasmids that expressed the *STE6* gene tagged with the hemagglutinin (HA) epitope tag. The *STE6* allele referred to as *STE6::HAe* (ecto-tagged) contains the epitope near the 5'-end of the gene, in the first extracellular loop of Ste6p, between amino acids 68 and 69 (Berkower *et al.*, 1994). The *STE6* allele referred to as *STE6::HAc* (C-terminally tagged) contains the epitope after the last amino acid of the Ste6p (Paddon *et al.*, 1996). The plasmids, pSM1080 and pSM1081, which contain ecto-tagged *ste6-90,166* and *ste6-166* (see below), were constructed as follows. The 3'-end of the *STE6* gene was amplified by PCR with two oligonucleotides, oSM161 and either oSM294 (to create pSM1080) or oSM295 (to create pSM1081). The sequence of the 5'-oligo oSM161 is 5'-CATTAAAATACGTAG-

GAATCC-3' and contains the wild-type *STE6* sequence, including a *Sna*BI site unique in the gene. The oligos oSM294 and oSM295 contain the mutations *ste6-90,166* and *ste6-166*, respectively. Both oligos create a *Hind*III site immediately downstream of the stop codon corresponding to the *ste6-166* mutation, which allowed subcloning of the PCR fragment into pSM693, a vector that contains *STE6::HAe*. The sequence of oSM294 is: 5'-GACCTCAAAGCTTATTCACCTATACAT-TATAACCATTGTTAGTAGAGCAGG-3', and of oSM295 is 5'-GACCTCAAAGCTTATTCACCTATGCGTTATAACC-3'.

Plasmid pSM955 was used to generate a strain with the *ste6-90* mutation integrated at the *STE6* locus. It harbors a *Spe*I-*Hind*III *STE6* fragment containing the 3'-end of the gene with the triple HA tag at the C terminus and the changes representing the *ste6-90* mutation cloned into a *Ylp URA3* vector (pRS306 [Sikorski and Hieter, 1989]). The plasmid pSM1083 was recovered from the mutagenesis of pSM683 and contains the *ste6-166* mutation. A *Sall*-*Hind*III fragment from pSM1083 subcloned into a *2 μ URA3* vector (pSM217) yielded pSM1082. To ascertain that one mutation conferred the hyperinstability and ER localization phenotypes associated with *ste6-166*, a *Bsu*36I-*Not*I fragment was subcloned into a fresh pSM683 plasmid, sequenced, and found to contain the *ste6-166* mutation reported in RESULTS. The resulting plasmid pSM1126 expressed a form of Ste6p that exhibited all the mutant phenotypes associated with the original plasmid obtained from the mutagenesis. Similarly, the high-copy plasmids pSM1086 and pSM1087, which contain the *ste6-13* and *ste6-90* mutations, respectively, were constructed by transferring the *Bsu*36I-*Not*I fragments into a fresh *STE6*-containing plasmid pSM672, which contains the HA tag at the C terminus. The low-copy plasmids pSM1084 and pSM1144, containing the *ste6-90* and *ste6-13*, respectively, were constructed by subcloning the *Sall*-*Not*I inserts from pSM1086 and pSM1087 into pRS316, a *CEN URA3* vector. The phenotypes resulting from the expression of Ste6p from the reconstructed plasmids are the same as those of the original mutant isolates.

Mating Assays

Quantitative mating assays were performed as previously described (Berkower and Michaelis, 1991), using the *MAT α* mating tester

SM1068. Qualitative patch-mating tests were performed as follows: The *ste6Δ* strain SM2544 was transformed with *URA3*-based plasmids carrying the wild-type or mutant versions of the *STE6* gene. Transformants were patched on a synthetic complete plate lacking uracil (SC-URA) plate and were allowed to grow for 2 d. The patches were then replica printed onto SD plates spread with a lawn of the *MATα* tester SM1068. Diploid formation was monitored after 2 d of growth on the diploid-selective plates at 30 or 37°C.

Screen to Identify ER-retained *ste6* Mutants

The in vitro hydroxylamine mutagenesis of pSM683 (*CEN URA3 STE6::HAe*) or pSM500 (2 μ *LEU2 STE6::HAe*) was performed as previously described (Kaiser *et al.*, 1994). The mutagenized DNA was transformed into *Escherichia coli* strain DH5 α . A population of transformant colonies was used to make a DNA preparation that was transformed into the yeast strain SM1563 (*ste6-Δ1::LEU2*) or SM1646 (*ste6-Δ2::URA3*). Transformants were initially screened for their mating capacity by a colony replica-plating assay. Of ~7500 transformants screened, we found 190 down-mater transformants that displayed various levels of mating defects. Of these, 32 isolates were screened by pulse-chase labeling for aberrant metabolic stability, yielding one mutant, *ste6-166*. From a separately mutagenized plasmid (pSM500), another set of 35 down-mater mutants was obtained and screened by immunofluorescence for aberrant localization of Ste6p to the ER, yielding two mutants, *ste6-13* and *ste6-90*. As described in RESULTS, *ste6-13* and *ste6-90* contain changes in two adjacent amino acids. The mutagen hydroxylamine usually generates single-transition mutations. The double mutations may have arisen due to extended treatment conditions (Sikorski and Boeke, 1991).

Mapping and Sequence Analysis of *ste6-13*, *ste6-90*, and *ste6-166*

The mating defect, aberrant localization, and aberrant stability associated with the *ste6-13*, *ste6-90*, and *ste6-166* alleles all mapped downstream of the *Bsu36I* site in the *STE6* gene, which lies at position 3532, 338 nucleotides upstream of the 3'-end of the coding sequence. For all three mutants, a *Bsu36I-NotI* fragment that contains the last 338 base pairs (bp) of the *STE6* coding sequence and the 3'-untranslated region was cloned into a fresh *STE6*-containing plasmid and shown to confer all three phenotypes. The region between the *Bsu36I* site and the stop codon of *STE6* was sequenced and found to bear the mutations described in RESULTS.

Antibodies

The 12CA5 mouse anti-HA monoclonal antibody was purchased from Babco (Richmond, CA). The rabbit anti-Kar2p antibody was a gift from M. Rose (Princeton University, Princeton, NJ). The 9E10 mouse anti-myc monoclonal antibody was obtained from the monoclonal antibody facility, Johns Hopkins University School of Medicine. Secondary rhodamine- or FITC-conjugated antibodies were purchased from Boehringer Mannheim (Indianapolis, IN), and the HRP-conjugated sheep anti-mouse secondary antibody was purchased from Amersham (Arlington Heights, IL).

Indirect Immunofluorescence

Cells were prepared as previously described (Berkower *et al.*, 1994). Cultures were grown overnight to an OD₆₀₀ of 0.5–1.0, and 5 OD₆₀₀ units were harvested and resuspended in 5 ml of KP buffer (0.1 M potassium phosphate, pH 6.5). A volume of 0.6 ml of a 37% formaldehyde solution (J.T. Baker, Phillipsburg, NJ) was added dropwise to the cell suspension, and fixation was allowed to occur for 40 min at 30°C with gentle agitation. Cells were washed twice in KP buffer and once in KPS buffer (KP buffer with 1.2 M sorbitol). For spheroplasting, 5 μ l of Zymolyase 20T (5 mg/ml) and 5 μ l of

β -mercaptoethanol were added to cells resuspended in 1 ml of KPS buffer. Cells were incubated 20 min at 30°C with gentle rotation. Cells were then harvested gently (2000 rpm in Beckman TJ-6 clinical centrifuge, 3 min) and washed once in 5 ml of KPS buffer. Finally, the cells were resuspended in 1 ml of KPS/0.1% Tween 20 and left at room temperature for 15 min.

For immunodetection, 15 μ l of the cell suspensions were applied to polylysine-coated slides and allowed to settle for 15 min. Wells were then washed once with PBST buffer (0.04 M K₂HPO₄, 0.01 M KH₂PO₄, 0.15 M NaCl, 10 mg/ml BSA, 0.1% NaN₃), and 15 μ l of primary antibody diluted in PBST buffer were applied overnight at room temperature. In all immunofluorescence experiments, Ste6p was detected using the 12CA5 (anti-HA) antibody (dilution 1:2000), and Kar2p was detected using polyclonal rabbit anti-Kar2p antibodies (dilution 1:1000). Secondary incubations were performed for at least 2 h at room temperature in the dark, using a rhodamine-conjugated anti-mouse antibody to detect 12CA5 and a FITC-conjugated anti-rabbit antibody to detect Kar2p (both at a dilution of 1:500). All antibody dilutions were made in PBST buffer. Wells were washed four times with PBST buffer between primary and secondary incubations.

Slides were mounted as described by Kaiser *et al.* (1994) and visualized using a Zeiss Axiovert (Carl Zeiss, Thornwood, NY) with a 100 \times objective. Images were captured on a 7100 PowerMac using the IP Lab Software (Scanalytics, Inc., Fairfax, VA), further processed with Adobe Photoshop, and printed on a dye-sublimation printer (Phaser 440, Tektronix, Wilsonville, OR).

Sucrose Gradient Fractionation

The fractionation of subcellular organelles was based on sedimentation through a sucrose step gradient essentially as described by Romano *et al.* (1998). Briefly, midlog cells expressing wild-type (SM2915) or mutant Ste6p (SM2916 and SM2917) were harvested, enzymatically converted to spheroplasts, and then osmotically lysed in buffer B (0.3 M Sorbitol, 10 mM triethanolamine, 1 mM EDTA, pH 7.2, containing 1 μ g/ml leupeptin and chymostatin, 2 μ g/ml pepstatin and aprotinin, and 1 mM PMSF). The lysate was homogenized, cleared twice by centrifugation (500 \times g) at 4°C to remove intact cells and debris, and then loaded on an 11-step sucrose gradient poured into a thin-walled SW28 ultracentrifuge tube. The gradient was composed of 3.4 ml layers of sucrose (18–54% [wt/vol] in 4% increments) layered over a 65% (wt/wt) sucrose pad (1.7 ml) with each step containing 10 mM HEPES, pH 7.5, and 1 mM MgCl₂. The gradients were centrifuged at 100,000 \times g for 2.5 h at 4°C in a SW28 rotor (Beckman, Fullerton, CA). Equivalent fractions (3.4 ml) were collected from the gradient after puncturing at the bottom of the ultracentrifuge tube with a 20-gauge needle.

All fractions were assayed for protein concentration and the distribution of marker enzyme activities as described by Romano *et al.* (1998). The relevant distribution of HA-tagged wild-type and mutant Ste6p in gradient fractions was determined by immunoblotting. Briefly, equivalent volumes (20 μ l) of each sucrose gradient fraction were solubilized with 6 \times sample buffer (150 mM Tris, pH 6.6, 6% SDS, 30% β -mercaptoethanol, 0.06% bromophenol blue), separated by SDS-PAGE (12.5%), and transferred at 200 mA onto nitrocellulose (Schleicher & Schuell, Keene, NH) for 15 h at 4°C. Blots were blocked, probed with anti-HA (1:5000), followed with HRP-conjugated goat anti-mouse secondary antibody (1:10,000), and immune complexes were detected by exposure to film after enhanced chemiluminescence detection (Boehringer Mannheim).

Metabolic Labeling and Immunoprecipitation of Ste6p

For metabolic labeling, cultures were grown for two to three doublings from OD₆₀₀ 0.2–0.75, after cells were diluted from a 2-d overnight culture. The cultures took 8–10 h to reach this stage. A total of 12.5 OD₆₀₀ units were harvested (2.5 OD₆₀₀ units per time

point) and resuspended in 2.5 ml of SD medium supplemented with appropriate amino acids. Cells were incubated with shaking at 30°C for 10 min and pulse labeled for 10 min with 75 μ Ci of Express ³⁵S (DuPont, Wilmington, DE). The label was chased by addition of 50 μ l chase mix (1 M cysteine, 1 M methionine), and samples (0.5 ml) were collected at 0, 15, 30, 60, and 90 min. The reaction was stopped by mixing cells with 0.5 ml stop mix (40 mM cysteine, 40 mM methionine, 20 mM NaN₃) in an Eppendorf tube on ice.

Total cell protein extracts for each time point were prepared as follows: cells were washed once and resuspended in 1 ml cold H₂O, lysed by adding 150 μ l of 2N NaOH/1 M β -mercaptoethanol, vortexed vigorously, and incubated on ice for 15 min. Trichloroacetic acid was added to 5%, and samples were left on ice an additional 15 min. Tubes were microfuged for 10 min, and protein pellets were resuspended in 50 μ l of trichloroacetic acid sample buffer (3.5% SDS, 0.5 M DTT, 80 mM Tris, 8 mM EDTA, 15% glycerol, 4 mg bromophenol blue).

Ste6-HA_p was immunoprecipitated from total extracts using the 12CA5 (anti-HA) antibody. For immunoprecipitation of Ste6_p, 25 μ l of extract were brought up to 0.5 ml with dilution buffer (1% Triton X-100, 150 mM NaCl, 5 mM EDTA, 50 mM Tris, pH 7.5) and incubated on ice for 60 min. The lysate was cleared twice to remove insoluble material, and 250 μ l of 12CA5 antibody dilution (final 12CA5 dilution was 1:1500) were added to the diluted protein. Incubation was allowed to proceed overnight at 4°C. Immune complexes were then pelleted using Protein A-Sepharose beads (Pharmacia Biotech, Piscataway, NJ). Immunoprecipitates were dissociated from the beads by the addition of 15 μ l of 2 \times Laemmli sample buffer and incubation at 37°C for 20 min. Immunoprecipitates were run on SDS-PAGE and analyzed by PhosphorImager (Molecular Dynamics, Sunnyvale, CA).

For determination of Ste6_p half-life, gels were analyzed by PhosphorImager. Counts corresponding to the Ste6_p signal were quantified in each lane using the ImageQuant software (Molecular Dynamics), and the 0 min chase time point was used as the 100% reference value for each individual time course experiment. Plotting on semilogarithmic graphs and exponential extrapolations were done using the KaleidaGraph Software (Synergy Software, Reading, PA).

Detection of Ubiquitinated Forms of Ste6_p

Unlabeled protein extracts for immunoprecipitation were prepared using the β -mercaptoethanol/NaOH extraction procedure as described above, except that 25 OD₆₀₀ of cells were harvested and *N*-ethylmaleimide (Sigma Chemical, St. Louis, MO) was present at a concentration of 10 mM throughout the preparation. The anti-HA antibody was used at a dilution of 1:750 in the immunoprecipitations. Immunoprecipitates were washed as described above, subjected to 8% SDS-PAGE (5 OD/lane), and transferred to nitrocellulose. For Western blots, anti-HA and anti-myc antibodies were used at dilutions of 1:10,000 and 1:3000, respectively, in the presence of 0.1% Tween 20. Immunoblots were developed using the ECL detection system (Amersham Life Sciences, Arlington Heights, IL).

Multicopy Suppressor Screen of *ste6-90*

To identify genes that could suppress the mating defect associated with *ste6-90* at high copy, a 2 μ *URA3* genomic library in YEp24 (created by M. Carlson) was transformed into SM2729, which contains the *ste6-90* allele integrated into the genome. Eighty five hundred primary transformants (corresponding to 4–5 genomes) were screened by colony mating for suppression of the *ste6-90* mating defect. A total of 22 candidates were rescreened and submitted to plasmid linkage analysis. Three candidates showed a higher level of mating, and suppression was shown to be linked to the 2 μ plasmid by retransformation. Two of the three plasmids, pSM1266 and pSM1267, contained an overlapping genomic region from chromosome VIII, with pSM1267 containing a smaller insert. The third plasmid was not pursued due to the weakness of the

suppression. The identification of the suppressing activity on the insert carried by pSM1267 was performed as follows: a *TthIII*A deletion of the plasmid, which removes the YHR027C and *PPA1* open reading frames (ORFs), was shown to eliminate the suppressing activity of pSM1267. The two remaining ORFs were inactivated by fill-in with *SacII* (to introduce a frameshift in YHR027C), or *AflII* (to introduce a frameshift in *PPA1*). The *SacII*-filled in plasmid lost suppressing activity, mapping the suppression activity to the YHR027C ORF. This ORF was previously designated *HRD2* (for HMG-CoA reductase degradation) by Hampton *et al.* (1996).

RESULTS

Three *Ste6_p* Mutant Proteins, *Ste6-13_p*, *Ste6-90_p*, and *Ste6-166_p*, Exhibit Aberrant ER Localization

We sought to identify mutant forms of Ste6_p that exhibited a defect in exit from the ER. To do so, we generated a collection of *ste6* mutants by in vitro plasmid mutagenesis, transformed these into a *ste6* Δ strain, and carried out a primary screen for mutants with reduced mating activity. Among the “down-maters,” we performed immunofluorescence and pulse-chase metabolic labeling as secondary screens to identify mutants in which Ste6_p exhibited an altered pattern of localization or metabolic stability,





Mutation	Patch Mating	Mating Efficiency (%)
<i>ste6-13</i>		42
<i>ste6-90</i>		0.4
<i>ste6-166</i>		0.05
<i>STE6</i>		100

Figure 1. Mating defects associated with the *ste6-13*, *ste6-90*, and *ste6-166* mutations. To assess the mating defect of the isolated *ste6* mutants, qualitative plate matings were carried out. Patches of *MATa* strains bearing plasmids that contain wild-type or mutant alleles of *STE6* were replica printed to a lawn of *MATa* cells spread on a diploid-selective plate. Quantitative mating tests were also performed, as described in MATERIALS AND METHODS, and the efficiency of diploid formation (expressed as a percentage of wild-type) is indicated to the right of the corresponding patch. The strains used are: SM2918 (*ste6-13*), SM2919 (*ste6-90*), SM3661 (*ste6-166*), and SM2914 (wild-type *STE6*). Strains express *STE6* from a 2 μ plasmid.

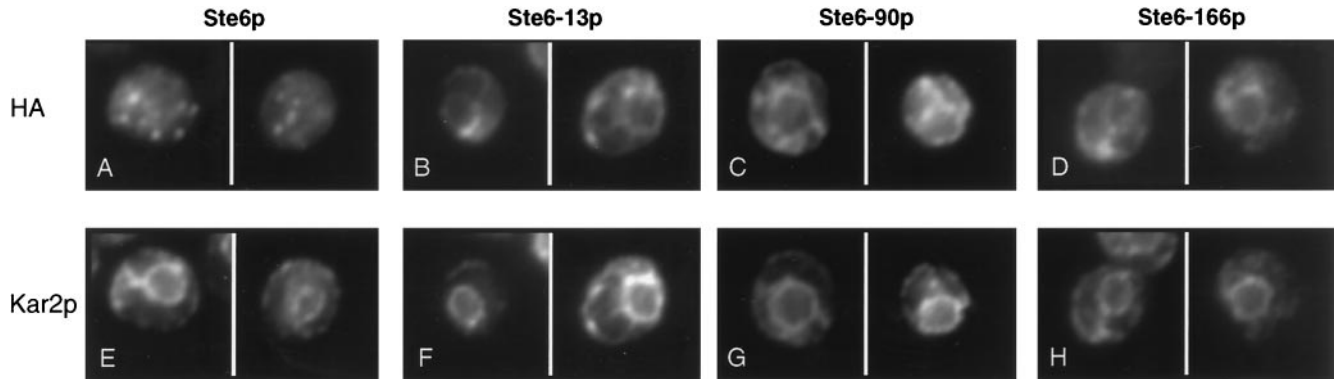


Figure 2. Three mutant forms of Ste6p are aberrantly ER localized by immunofluorescence. The localization of wild-type and mutant forms of Ste6-HA_p was examined by coimmunofluorescence with the ER marker Kar2p. The pattern of Ste6p localization is revealed by staining with the anti-HA antibody (A–D, top panels), and the position of the ER in the same cells is detected by staining with an antibody to the ER marker Kar2p (E–H, bottom panels). The secondary antibodies, a Rhodamine-conjugated anti-mouse and FITC-conjugated anti-rabbit, were used to detect Ste6-HA_p and Kar2p, respectively. Strains used were the same as in Figure 1. It should be noted that the wild-type and mutant *ste6* gene products are expressed from a high-copy number (2μ) plasmid, resulting in variability of staining from cell to cell. Consistent with a significant decrease in the metabolic stability of Ste6–166p (see Figure 3), the proportion of cells harboring this mutant protein that exhibit detectable immunofluorescence was considerably lower than for wild-type Ste6p or for the Ste6–13p and Ste6–90p mutant proteins. For clarity, examples of the brightest staining cells are shown for Ste6–166p.

respectively (see MATERIALS AND METHODS), since both assays can identify trafficking aberrations of Ste6p. Of 67 mating-defective mutants, 3 exhibited an ER retention phenotype, as described below.

The mating defect of the mutants varies over a broad range. The *ste6–90* and *ste6–166* alleles support only very low levels of mating (0.4 and 0.05% of wild-type, respectively), whereas the *ste6–13* allele displays an intermediate phenotype (42% of wild-type) (Figure 1). By immunofluorescence, all three mutant proteins exhibit a perinuclear ER-staining pattern, in contrast to the punctate Golgi-staining pattern of wild-type Ste6p (Figure 2, compare panels B, C, and D to A) (Berkower *et al.*, 1994; Loayza and Michaelis, 1998). The position of the ER was confirmed by coimmunofluorescence with the well-established ER marker Kar2p (Figure 2, bottom panels). Thus, it appears that all three mutant proteins are defective for efficient exit from the ER. Their low level of functional activity, as measured by the mating assay, may result from aberrant trafficking, abnormal structure, or both. The residual mating activity conferred by these mutant proteins is likely to result from a low level of mutant protein exiting the ER.

To independently confirm the ER localization of the Ste6p mutant alleles, we carried out subcellular fractionation. Total cell lysates from cells expressing wild-type or two mutant forms of Ste6p (Ste6–13p and Ste6–90p) were subjected to sucrose gradient fractionation and assayed for marker enzymes. As shown in Figure 3, cytosol does not enter the gradient as indicated by the high concentration of protein at the top of the three gradients. Several enzymatic activities fractionate with light membranes in the

upper half of the gradient (fractions 1–5). These include vacuolar (α -D-mannosidase), *trans*-Golgi network (Kex2p), and Golgi activities (GDPase). Both the ER marker activity (NADPH cytochrome *c* reductase) and plasma membrane marker activity (ATPase) fractionate with heavy membranes in the lower half of the gradient. The ER marker NADPH cytochrome *c* reductase activity peaks in fractions 8, whereas plasma membrane ATPase activity peaks in fraction 9.

We determined by immunoblotting that wild-type Ste6p is localized to the upper half of the gradient, consistent with our previous report that the steady-state localization of Ste6p is to a membrane compartment that contains Kex2p (Loayza and Michaelis, 1998). The distributions of the Ste6–13p and Ste6–90p, however, were distinct from that of wild-type Ste6p. These mutant forms of Ste6p were localized to the bottom half of their respective gradients, both with peaks in fraction 8. This fractionation pattern is most similar to that of NADPH cytochrome *c* reductase and supports our contention that Ste6–13p and Ste6–90p are ER-retained. Taken together, the immunofluorescence and the fractionation pattern of Ste6–13p and Ste6–90p show a steady-state localization in the ER that could be viewed either as a strong kinetic delay in exit from the ER or as active retention. In either case, a small fraction of the mutant proteins could exit or escape the ER and account for the signal detected in the lighter portion of the gradient. Due to the rapid turnover of Ste6p-166 (see below), a similar fractionation analysis was not performed.

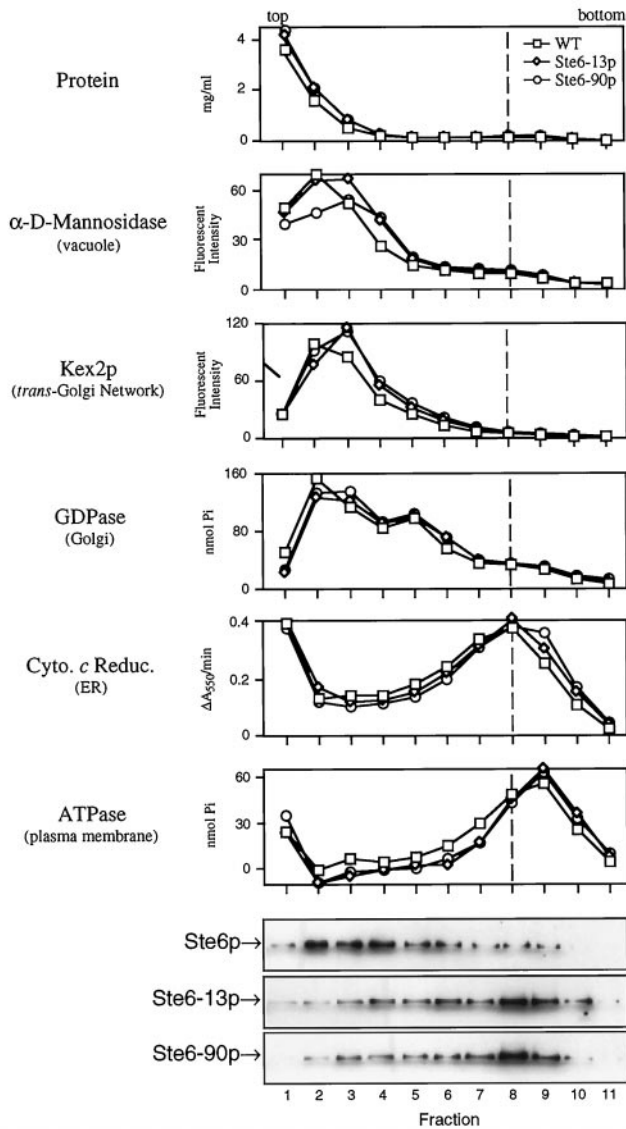


Figure 3. Sucrose gradient fractionation of wild-type and ER-retained mutant forms of Ste6p. Total yeast lysates prepared from wild-type and mutant strains were subjected to sucrose gradient fractionation as described in MATERIALS AND METHODS. Fractions from the gradient were collected and assayed for the distribution of total protein and marker enzymes. The distribution of Ste6p, Ste6-13p, and Ste6-90p was determined by immunoblotting with the anti-HA antibody and an HRP-conjugated sheep anti-mouse secondary antibody, followed by enhanced chemiluminescent detection. The dashed line indicates the peak of ER microsomes as defined by NADPH cytochrome *c* reductase activity. Strains used are SM2544 ($\Delta ste6$) transformed with *CEN* plasmids bearing either wild-type Ste6p (pSM1085), Ste6-13p (pSM1144), or Ste6-90p (pSM1084), each tagged with the HA epitope.

Ste6-13p, Ste6-90p, and Ste6-166p Represent Two Mutant Classes, Based on Their Distinct and Aberrant Metabolic Stability

The relatively short metabolic half-life of wild-type Ste6p (~20 min) is due to its constitutive endocytosis

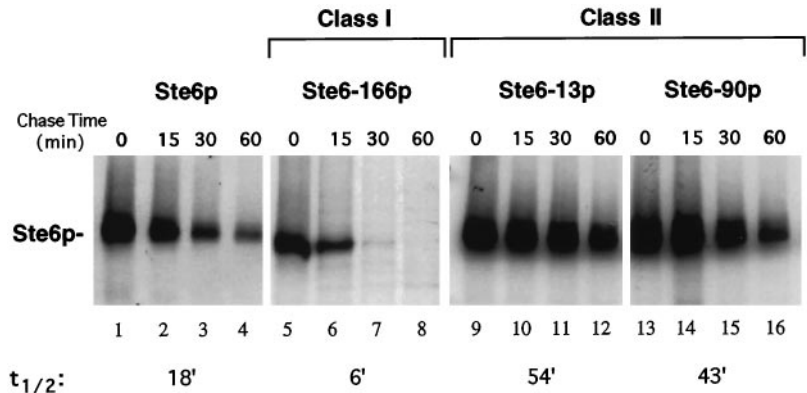
from the plasma membrane, followed by delivery to and degradation within the vacuole (Berkower *et al.*, 1994; Kölling and Hollenberg, 1994). Therefore, the failure of Ste6p to reach the vacuole, as would be the case for an ER-retained Ste6p mutant, should be reflected in a difference in the kinetics of its degradation. To assess the rate of degradation of our ER-localized Ste6p mutant proteins, we carried out pulse-chase analysis (Figure 4). The mutants clearly fall into two categories. The half-life of Ste6-166p (lanes 5-8) is significantly shorter than that observed for wild-type Ste6p (lanes 1-4), 6 min versus 18 min, respectively, which corresponds to a threefold faster rate of degradation for Ste6-166p. In contrast, the half-lives of Ste6-13p (lanes 9-12) and Ste6-90p (lanes 13-16) are 54 min and 43 min, respectively, which are considerably longer (2.5- to 3-fold) than the 18-min half-life of wild-type Ste6p. Thus, although the three ER-retained *ste6* mutants appear indistinguishable by immunofluorescence, their half-lives define distinct classes.

We have designated the hyperunstable Ste6-166p allele as a "Class I" mutant and the hyperstable alleles, Ste6-13p and Ste6-90p, as "Class II" mutants, based on their distinctive and abnormal metabolic degradation patterns, as compared with wild-type Ste6p. It is notable that the half-lives of the Class II mutants, Ste6-13p and Ste6-90p, are quite similar to one another, yet their mating efficiencies differ by nearly 100-fold (42% and 0.4%, respectively). It is likely that the *ste6-90* mutation severely impairs function, in addition to affecting localization of the mutant protein, so that any fraction of mutant protein that does manage to escape the ER would function very poorly as an *a*-factor transporter.

Sequence of the ste6-13, ste6-90, and ste6-166 Mutations

We mapped the mutations responsible for the Class I and Class II mutant phenotypes to a 50-residue segment of Ste6p that contains the Walker B site (Figure 5A) and is located within or adjacent to the C-terminal NBD of Ste6p (see MATERIALS AND METHODS for details). This region of Ste6p is predicted to be cytosolically oriented (Kuchler *et al.*, 1989; Geller *et al.*, 1996). DNA sequence analysis indicates that the Class I mutant *ste6-166* bears a premature termination mutation (Q1249X). The Ste6-166p protein is therefore 42 amino acids shorter than wild-type Ste6p, or about 4.6 kDa smaller, a size difference that is detectable by SDS-PAGE (see Figure 4). The two Class II mutants, *ste6-13* and *ste6-90*, each contain an adjacent pair of missense mutations (A1201T, R1202I; and T1245M, H1246Y, respectively) (Figure 5B). As shown in the alignment in Figure 5B, the residues altered in both mutants lie in a conserved region in or near the N- and C-terminal NBDs of other ABC proteins (MDR, CFTR,

Figure 4. Ste6-13p, Ste6-90p, and Ste6-166p define two classes based on aberrant metabolic stability. The metabolic stability of ER-localized *ste6* mutants was examined by pulse-chase analysis. Cells were pulse-labeled for 10 min with Express³⁵S, and the label was chased for the indicated times (min). Wild-type and mutant forms of Ste6-HAP were immunoprecipitated from total extracts with the anti-HA antibody, and immunoprecipitates were analyzed by SDS-PAGE on 8% gels. Bands were detected and quantified by PhosphorImager analysis using Imagequant software. The Ste6p half-life ($t_{1/2}$) is indicated at the bottom of each panel. Strains were the same as in Figure 1.



and Ste6p). The fact that all three mutations fall strikingly close together, particularly considering the large size of Ste6p (1290 amino acids), suggests that this particular region of Ste6p may play a critical role in exit from the ER.

The amino acid changes, A1201T and R1202I (the changes corresponding to *ste6-13*) and T1245M and H1246Y (the changes corresponding to *ste6-90*), were generated as single-point mutations in *STE6*. We found that the amino acid change R1202I had a phenotype similar to the *ste6-13* mutation, although its defect was not as pronounced. The R1202I mutant protein supported mating to 60%, showed ER localization, and was also hyperstable, with a half-life of 37 min. For *ste6-90*, both amino acid changes were required for the phenotypes described.

The Degradation of Ste6-166p Does Not Occur in the Vacuole, but Instead Takes Place Before Exit from the ER

The degradation of wild-type Ste6p involves vacuolar proteases whose activities depend on the master vacuolar protease Pep4p. The hyperunstable phenotype of Ste6-166p could be due to its faster rate of arrival in the vacuole, or to the involvement of nonvacuolar proteolytic machinery. To determine whether Ste6-166p is degraded in the vacuole or elsewhere, we examined its half-life in a *pep4Δ* mutant. Unlike wild-type Ste6p, which is stabilized in the *pep4Δ* mutant (Figure 6, top and middle left panels, lanes 1-4), Ste6-166p undergoes degradation with an identical rate in the *pep4Δ* mutant and the isogenic wild-type *PEP4*⁺ strain (Figure 6, top and middle right panels, lanes 5-8); this Pep4p-independent degradation suggests that Ste6-166p does not reach the vacuole.

To address whether the rapid degradation of Ste6-166p occurs before its exit from the ER, we examined the fate of Ste6-166p in the *sec18-1* mutant, which exhibits an ER to Golgi vesicular trafficking defect at 37°C (Novick *et al.*, 1981). Wild-type Ste6p is stabilized

when the *sec18-1* mutant is shifted to restrictive temperature (Figure 6, bottom left panel), since it is unable to reach the vacuole under these conditions (Berkower *et al.*, 1994; Kölling and Hollenberg, 1994). In contrast, the hyperinstability of Ste6-166p is unaffected in the *sec18-1* mutant at restrictive temperature (Figure 6, bottom right panel). We conclude that the degradation of Ste6-166p does not require its exit from the ER. Instead, Ste6-166p appears to be degraded before the ER-to-Golgi transition, possibly in situ in the ER membrane.

The Degradation of Ste6-166p Requires the Ubiquitin-conjugating Enzymes, Ubc6p and Ubc7p, and the Activity of the Proteasome

Since the vacuolar proteolytic system is not involved in the degradation of Ste6-166p, a likely alternative is the ubiquitin-proteasome system. We therefore tested whether mutations in genes encoding components of ubiquitin-proteasome pathway affected the degradation rate of Ste6-166p. As shown in Figure 7, Ste6-166p is stabilized significantly in the *ubc6,7Δ* double mutant, which is defective for a specific pair of ubiquitin-conjugating enzymes that reside in the ER membrane (Chen *et al.*, 1993; Sommer and Jentsch, 1993). The half-life of Ste6-166p in the *ubc6,7Δ* strain is approximately 10-fold greater than in the wild-type strain (57 min vs. 6.5 min, respectively), (Figure 7, compare lanes 5-8 to 1-4). Thus, a defect in ubiquitination correlates with a defect in the degradation of Ste6-166p, implicating the ubiquitin-proteasome system in the rapid turnover of the mutant protein.

To further analyze cellular components that could be required for the degradation of Ste6-166p, we determined the half-life of Ste6-166p in the *doa4Δ* mutant, in which a deubiquitination enzyme is altered and the activity of the proteasome is compromised (Papa and Hochstrasser, 1993). Ste6-166p is stabilized in this mutant over a time course of 60 min (Figure 7, lanes 9-12), as strongly as observed for the *ubc6,7Δ*

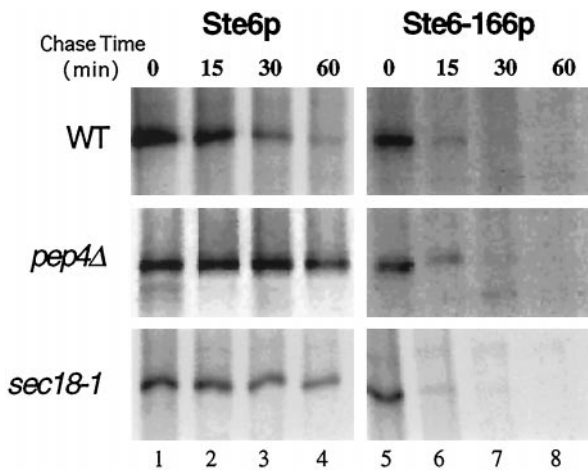


Figure 6. The degradation of Ste6-166p is not affected in *pep4Δ* or *sec18-1* mutants. The metabolic stability of wild-type Ste6p and Ste6-166p was examined in wild-type, *pep4Δ*, and *sec18-1* strains. Cells were pulse-labeled for 10 min with Express³⁵S, and the label was chased for the indicated times (min). Immunoprecipitations, detection, and quantification of the bands were performed as described in the legend to Figure 4 and in MATERIALS AND METHODS. The labeling of the *sec18-1* mutant was performed after a 40-min preincubation at restrictive temperature (37°C). The isogenic wild-type *SEC18* strain was submitted to the same temperature shift and showed no significant difference in the degradation of Ste6-166p (our unpublished result). The imposition of the block was confirmed by examining CPY processing in the same extracts. The p1 (ER glycosylated) form of CPY accumulated in the *sec18-1* mutant at restrictive temperature, confirming the ER-to-Golgi block. The p2 form of CPY accumulated and mature CPY was absent in the *pep4Δ* mutant, confirming the defect in vacuolar proteolysis (our unpublished results). Strains used were SM3663 (*PEP4* [*CEN STE6::HAe*]), SM3664 (*PEP4* [*CEN ste6-166::HAe*]), SM3665 (*pep4Δ* [*CEN STE6::HAe*]), SM3666 (*pep4Δ* [*CEN ste6-166::HAe*]), SM3662 (*sec18-1* [*CEN STE6::HAe*]), and SM2807 (*sec18-1* [*CEN ste6-166::HAe*]).

1993). As shown in Figure 8B, treatment with MG132 leads to significant stabilization of Ste6-166p, about fourfold relative to the mock treatment with DMSO only (although Ste6-166p has a somewhat longer half-life in the *erg6Δ* strain background than in the other strains used in this study), confirming the notion that the proteasome is responsible for the degradation of Ste6-166p in the ER.

Figure 7. Ste6-166p is stabilized in mutants defective in the ubiquitin-proteasome degradation pathway. The metabolic stability of Ste6-166p was examined by pulse-chase analysis as described in Figure 4. Strains used were SM3627 (wild-type [*CEN ste6-166::HAe*]), SM3667 (*ubc6,7Δ* [*CEN ste6-166::HAe*]), and SM2734 (*doa4Δ* [*CEN ste6-166::HAe*]).

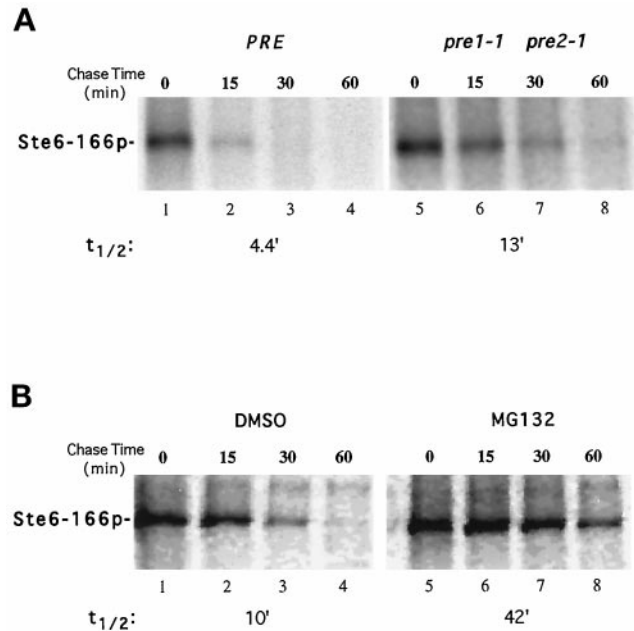
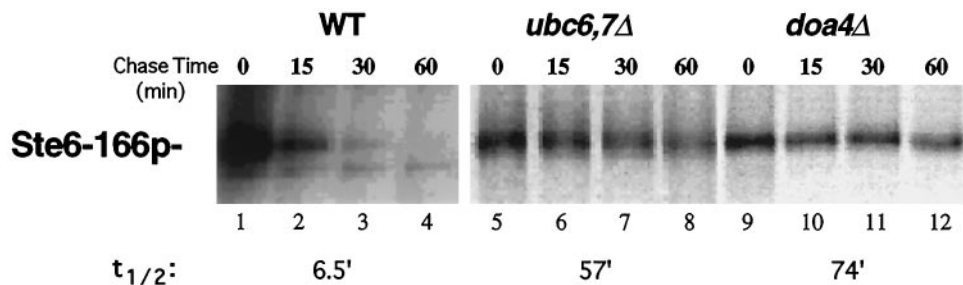


Figure 8. Degradation of Ste6-166p requires the activity of the 20S proteasome. The metabolic stability of Ste6-166p was examined by pulse-chase analysis as described in Figure 4. (A) The labeling of the *pre1-1 pre2-1* mutant and the isogenic wild-type strains was performed after a 40-min preincubation at 37°C. Strains were SM3289 (wild-type [*CEN ste6-166::HAe*]) and SM3291 (*pre1-1 pre2-1* [*CEN ste6-166::HAe*]). (B) To assess the effect of the proteasome inhibitor MG132 on the degradation of Ste6-166p, cells were pretreated with 50 μ M MG132 in DMSO or DMSO only for 1 h before labeling. The strain used was SM3599 (*erg6Δ* [*CEN ste6-166::HAe*]).

Ste6-166p Remains in the ER, Even When It Is Not Efficiently Degraded

It is possible that reduced degradation of Ste6-166p would allow it to exit the ER. To examine this possibility, we determined the localization of Ste6-166p under conditions in which it is not efficiently degraded, i.e., in the *ubc6,7Δ* and in the *doa4Δ* mutants (Figure 7). The perinuclear immunofluorescence localization pattern of Ste6-166p in the *ubc6,7Δ* and *doa4Δ* mutants is indistinguishable from that of Kar2p, indicating that Ste6-166p is still localized to the ER (Figure 9), even when it is not efficiently degraded. Thus,

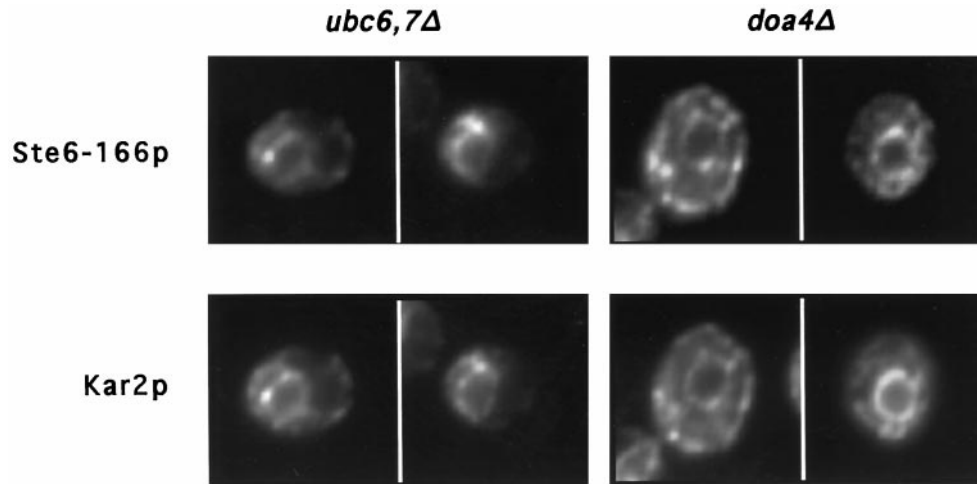


Figure 9. Ste6-166p does not exit the ER, even under conditions in which it is stabilized. The localization of Ste6-166p was examined by immunofluorescence in mutants defective in the ubiquitin-proteasome pathway. In the top panels, Ste6-166p is detected with the anti-HA antibody. In the bottom panels, the location of the ER in the same cells is determined by coimmunofluorescence with the anti-Kar2p antibody. The secondary antibodies used to detect Ste6-HA and Kar2p, respectively, were Rhodamine-conjugated anti-mouse and FITC-conjugated anti-rabbit. Strains are SM3032 (*ubc6, 7Δ* [2μ *ste6-166::HAe*]) and SM2731 (*doa4Δ* [2μ *ste6-166::HAe*]).

inhibition of the degradation of Ste6-166p in the ER does not alleviate its trafficking defect. Therefore, in the *ubc6,7Δ* and *doa4Δ* mutants, the Class I mutant protein Ste6-166p acts as a phenocopy of the Class II mutant proteins, Ste6-13p and Ste6-90p, in that it is ER-retained and hyperstable.

Ste6-166p Is Ubiquitinated

Since the ubiquitin-proteasome degradation pathway appears to be responsible for the rapid degradation of the Class I mutant, Ste6-166p, we asked whether we could detect ubiquitinated forms of it. We also examined the Class II mutant, Ste6-13p. We used a strain harboring a myc-tagged ubiquitin gene expressed from a high-copy plasmid. Ste6-HA was immunoprecipitated from total extracts and subjected to SDS-PAGE. Proteins were transferred to a nitrocellulose membrane, which was probed by immunoblotting with the anti-myc (9E10) antibody to detect ubiquitinated species of Ste6-166p. This assay is described by Hochstrasser *et al.* (1991). We and others have used this assay to detect ubiquitinated forms of wild-type Ste6p (Figure 10, lane 1), for which ubiquitination presumed to occur at the cell surface appears to be a prerequisite for endocytosis (Kölling and Hollenberg, 1994; Kölling and Losko, 1997; Loayza and Michaelis, 1998).

As shown in Figure 10, the Class I and Class II mutants, Ste6-166p and Ste6-13p, respectively, exhibit strikingly different levels of ubiquitination from one another. Ubiquitinated forms of Ste6-166p are present at a higher level than that seen for Ste6-13p (Figure 10A, compare lanes 3 and 2), despite the much lower steady-state protein level of Ste6-166p as compared with wild-type Ste6p or Ste6-13p (Figure 10B, compare lane 3 to lanes 1 and 2). The low steady-state amount of Ste6-166p reflects its hyperinstability. We

conclude that the defect displayed by Ste6-166p in the ER results in the ubiquitination of the mutant protein, which in turn leads to rapid degradation by the ubiquitin-proteasome degradation system. This outcome does not result simply from a defect in exiting the ER, since it is not observed with Ste6-13p. It should be noted that ubiquitination of wild-type Ste6p (Figure 10, lane 1) presumably occurs at the cell surface before endocytosis, and thus may occur via a completely different mechanism from that responsible for the ERAD of ER-retained mutant form of Ste6p. Thus, ubiquitination of Ste6p may have different consequences depending on where (ER vs. plasma membrane) and how it occurs.

The Hyperinstability of Ste6-166p Predominates over the Hyperstability of Ste6-90p

Since we identified two classes of *ste6* mutants defective for efficient exit from the ER, we wanted to know which class would predominate over the other phenotypically. To address this question, we generated a mutant form of *STE6* that contained the changes that correspond to *ste6-90* in combination with the *ste6-166* mutation (Figure 5B). This double-mutant allele of *STE6* is designated *ste6-90,166*. As shown in Figure 11, Ste6-90,166p shows the same hyperunstable phenotype as Ste6-166p (lanes 9–12 and 13–16). Thus, the hyperunstable phenotype associated with *ste6-166* predominates over the hyperstable phenotype seen with *ste6-90*.

HRD2 Is an Allele-specific High-Copy Suppressor of the Mating Defect Associated with ste6-90 and ste6-166

To identify cellular components that may allow ER-retained mutant forms of Ste6p to exit the ER, we

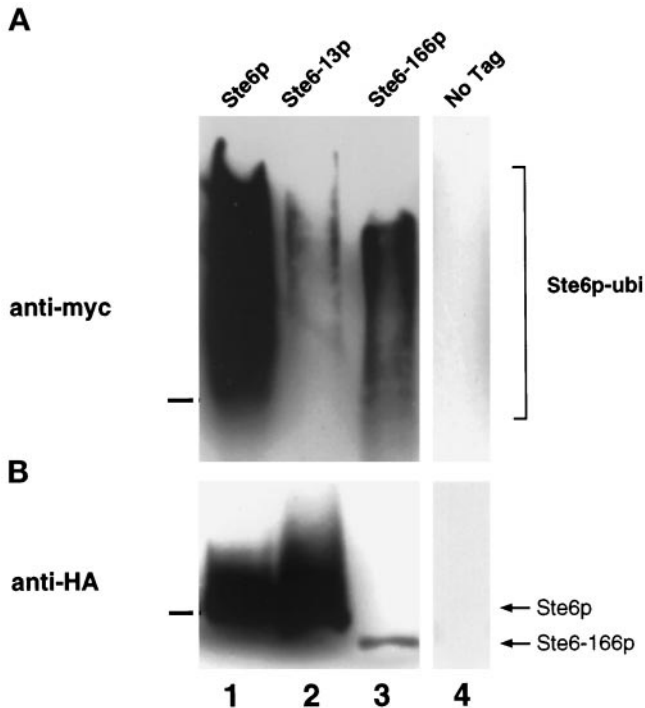


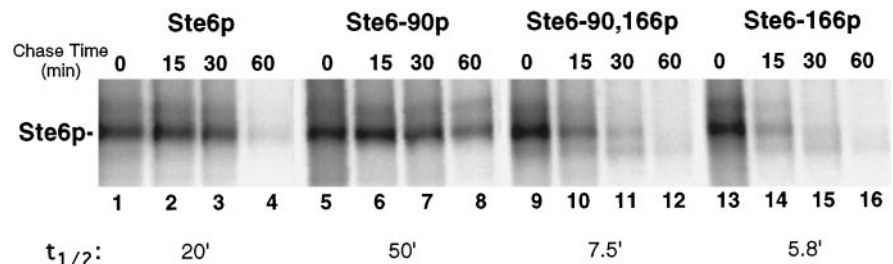
Figure 10. Ubiquitination of wild-type and mutant forms of Ste6p. Strains expressing *STE6::HA* and myc-tagged ubiquitin were used to examine the extent of ubiquitination of various forms of Ste6p. Protein extracts prepared from these strains were subjected to immunoprecipitation with the 12CA5 (anti-myc) antibody to immunoprecipitate Ste6p. The immunoprecipitates were separated on a 8% SDS gel and transferred to nitrocellulose. (A) The membrane was probed with the 9E10 (anti-myc) antibody to detect ubiquitinated forms of Ste6p. (B) The membrane was stripped and reprobed with the anti-HA antibody to detect total amounts of Ste6p present in the extracts. The bar at left indicates identical positions on panels A and B. Strains are SM3548 ($[2\mu STE6::HA, 2\mu ubi::myc]$), SM3668 ($[2\mu ste6-13::HA, 2\mu ubi::myc]$), SM3550 ($[2\mu ste6-166::HA, 2\mu ubi::myc]$), and SM3669 ($[2\mu STE6 (untagged), 2\mu ubi::myc]$).

initiated a multicopy suppressor screen of the mating defect associated with *ste6-90*. A 2μ genomic library was transformed into a strain containing the *ste6-90* allele integrated into the genome. Of 8500 transformants screened, 2 showed a 10-fold increase in mating that was plasmid-linked. Restriction mapping indi-

cated that these were independent isolates containing nonidentical, but overlapping, genomic inserts. Mapping of the region that conferred suppression (described in MATERIALS AND METHODS) indicated that the ORF *YHR027C* encodes the activity that suppresses the mating defect associated with the *ste6-90* mutation (Figure 12A). We also examined a panel of *ste6* loss-of-function mutants for suppression (Figure 12B). Interestingly, this analysis revealed that in addition to *ste6-90*, high-copy number *YHR027C* could suppress the mating defect of *ste6-166*, but not that of the other trafficking allele, *ste6-13*, nor of nontrafficking loss-of-function alleles, including *ste6-K398R*, *ste6-K1093R*, *ste6-G509D*, or *ste6-G1193D*, which alter the NBDs of Ste6p (Berkower and Michaelis, 1991) (Figure 12, A and B). Thus, suppression of a *ste6* mating defect by $2\mu YHR027C$ is not a general phenomenon, but is seen only for certain *ste6* trafficking alleles and, in particular, only for two alleles that map very close to one another.

The ORF *YHR027C* corresponds to the previously identified gene *HRD2*. The predicted sequence for Hrd2p shows high homology with p97, a mammalian subunit of the 19S cap of the proteasome, the regulatory complex of the 26S proteasome (Hampton *et al.*, 1996; Tsurumi *et al.*, 1996). *HRD2* was identified based on its being required for the regulated degradation of the enzyme HMG-CoA reductase in the ER (Hampton *et al.*, 1996). The suppression by $2\mu HRD2$ of the mating defects of Ste6-90p and Ste6-166p is likely to occur by an increase in the ER exit of these Ste6p mutant proteins. We did not observe an increased half-life or increased cell surface staining in an *end4* mutant for either mutant (our unpublished results). However, because of the high degree of sensitivity of the mating test versus the low degree of sensitivity of immunofluorescence, moderately improved mating may be easier to detect than moderately improved exit of Ste6p from the ER. While the mechanism of suppression of the mating defect associated with Ste6-166p and Ste6-90p remains to be elucidated, the identification of *HRD2* as a suppressor suggests that there may be a connection between the regulated degradation of a wild-type ER protein (HMG-CoA reductase)

Figure 11. The double mutant *ste6-90,166* exhibits the same hyperunstable phenotype as the single mutant *ste6-166*. To compare the effect of the double mutation *ste6-90,166* with the single mutations *ste6-90* and *ste6-166*, we examined the metabolic stability of Ste6p encoded by these alleles by performing pulse-chase analysis, as described in Figure 4. Strains are SM2569 ($[2\mu STE6::HAe]$), SM2919 ($[2\mu ste6-90::HAe]$), SM3154 ($[2\mu ste6-90/166::HAe]$), and SM3156 ($[2\mu ste6-166::HAe]$).



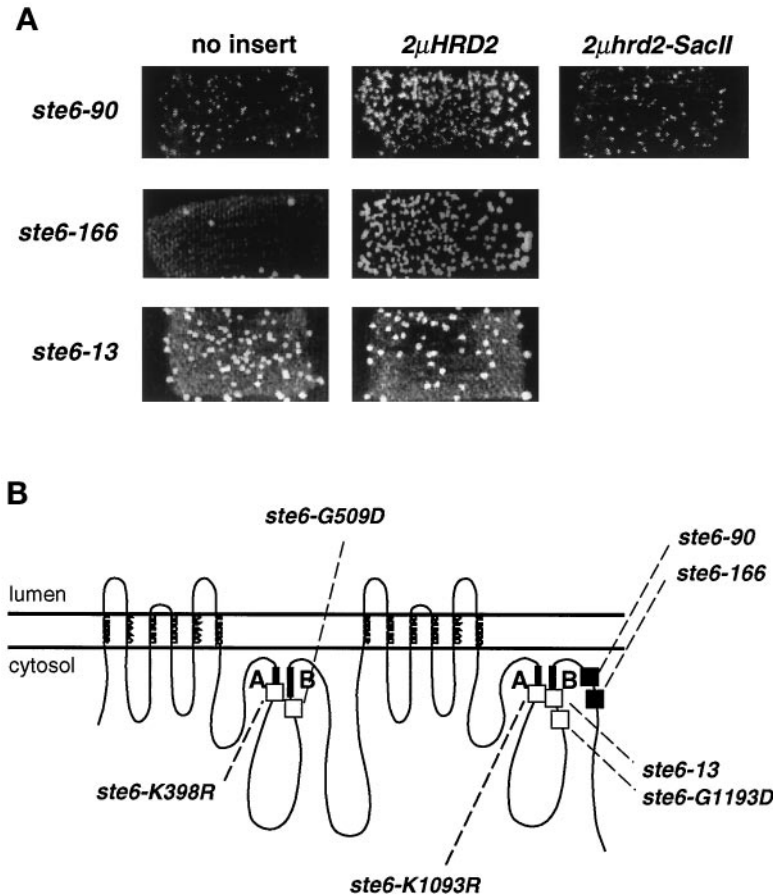


Figure 12. *HRD2* is a multicopy suppressor of the mating defect associated with *ste6-90* and *ste6-166*. (A) Qualitative patch matings were performed on a strain bearing the *ste6-90* mutation integrated in the genome (top row) and carrying a 2 μ plasmid with no insert (left panel), *HRD2* (middle panel), or *HRD2* filled in at the unique *SacII* site (right panel). Diploids were selected as described in MATERIALS AND METHODS and in the legend to Figure 1. As a comparison, the effect of 2 μ *HRD2* with *CEN ste6-166* or integrated *ste6-13* is shown (middle and bottom row, respectively). Strains are: SM3460 (*ste6-90*/vector only), SM3479 (*ste6-90* [2 μ *HRD2*]), SM3674 (*ste6-90* [2 μ *HRD2* filled in]), SM3488 ([*CEN ste6-166*]/vector only), SM3486 ([*CEN ste6-166*]/[2 μ *HRD2*]), SM3461 (*ste6-13*/vector only), and SM3884 (*ste6-13*/[2 μ *HRD2*]). (B) High-copy *HRD2* does not suppress other *ste6* alleles. The relative positions of the *ste6* mutations tested are indicated on the topological diagram of Ste6p. The open squares represent *ste6* alleles that are not suppressed by multicopy *HRD2*, and the black squares are alleles that can be suppressed by *HRD2*.

and the folding or degradation of an ER-retained mutant membrane protein (Ste6p).

DISCUSSION

Two Classes of Ste6p Mutant Proteins with a Defect in Exit from the ER

The overall goal of this study was to identify mutant forms of Ste6p, the α -factor transporter in *S. cerevisiae*, that would be substrates for the ER quality control system. We presently know little about the ER quality control system in yeast. In particular, few studies have dealt with how aberrant multispanning membrane proteins are recognized and handled by this system. By screening a collection of loss-of-function *ste6* mutants, we isolated three mutants, Ste6-13p, Ste6-90p, and Ste6-166p, that are defective in efficient exit from the ER. Whereas in all three cases the mutant proteins fail to exit the ER, we show that they define two distinct phenotypic classes on the basis of their metabolic half-lives. The Class I mutant, Ste6-166p, is highly unstable and behaves as a prototypical substrate for ERAD. In contrast, the Class II mutants,

Ste6-13p and Ste6-90p, do not appear to be substrates for ERAD; they are hyperstable, undergoing little degradation over time. To our knowledge, this represents the first report of a single protein in yeast for which distinct mutant forms can be channeled to different outcomes by the ER quality control system; our study suggests a model for a linear pathway of ER quality control comprised of at least two distinct checkpoints, as discussed below.

Because the degradation of a misfolded multispanning membrane protein is only poorly characterized in yeast, we analyzed several features of the metabolic instability of the Class I mutant Ste6-166p. We found that its degradation displayed many features in common with other ERAD substrates. In contrast to wild-type Ste6p, the half-life of Ste6-166p is unaffected in a *pep4* or *sec18* mutant, indicating that the degradation of Ste6-166p does not occur in the vacuole, nor does it require vesicular trafficking out of the ER. Instead, the rapid degradation of Ste6-166p is promoted by the ubiquitin-proteasome system, since strains defective in an ER-associated pair of ubiquitin-conjugating enzymes (*ubc6*, 7), or in the activity of the 26S protea-

some (*pre1*, 2 or *doa4*), cannot efficiently degrade it. Furthermore, Ste6-166p is significantly spared from degradation *in vivo* after treatment of cells with the proteasome inhibitor MG132. Thus, similar to previously reported ERAD substrates in yeast, including mutant forms of soluble proteins (CPY* and pro- α -factor) (Hiller *et al.*, 1996; McCracken and Brodsky, 1996) and a membrane protein (Sec61-2p) (Biederer *et al.*, 1996), the degradation of Ste6-166p is proteasome-dependent. Likewise, in mammalian cells, the proteasome mediates the ER degradation of wild-type and mutant forms of the multispanning membrane protein CFTR.

It has been suggested that aberrant proteins are reverse translocated from the ER lumen or ER membrane into the cytosol before their degradation, as has been shown for the mammalian single-pass membrane protein MHC class I heavy chain (Wiertz *et al.*, 1996; Hughes *et al.*, 1997) and for the soluble yeast pro- α -factor (McCracken and Brodsky, 1996). However, we have found that Ste6-166p sediments with the membrane fraction, even under conditions where the proteasome activity is inhibited (our unpublished results), suggesting that it is degraded *in situ* at the cytoplasmic surface of the ER membrane. It is perhaps not surprising that the cytosolic proteasome can degrade a mutant form of Ste6p without its removal from the membrane since most portions of Ste6p, with the exception of short luminal loops and the membrane spans *per se*, are predicted to reside on the cytosolic face of the ER membrane and thus could be directly accessible to the proteasome. We note, however, that we cannot dismiss the possibility that Ste6-166p does enter the cytosol but forms cytosolic aggregates, so that its apparent cosedimentation with membranes upon treatment with proteasome inhibitors is fortuitous.

In contrast to the instability of the Class I mutant, the Class II mutants, Ste6-13p and Ste6-90p, are hyperstable, exhibiting little degradation over time. The inefficient exit of Ste6-13p and Ste6-90p from the ER could involve a mechanism destined to allow more time for defective proteins to fold correctly or to bind appropriate folding or chaperone factors, ultimately permitting at least a fraction of the protein to resume normal trafficking. Such a trafficking defect resembles that documented in mammalian cells for the temperature-sensitive mutant VSV G tsO45 protein, when cells are incubated at the nonpermissive temperature (Doms *et al.*, 1987).

It is notable that the Class I allele Ste6-166p is a premature termination codon resulting in the production of a truncated form of Ste6p, whereas the Class II alleles are missense mutants. Nevertheless, the type of mutation does not dictate the class, since other truncated *ste6* mutants isolated in this laboratory (Nijbroek and Michaelis, unpublished results) produce metabol-

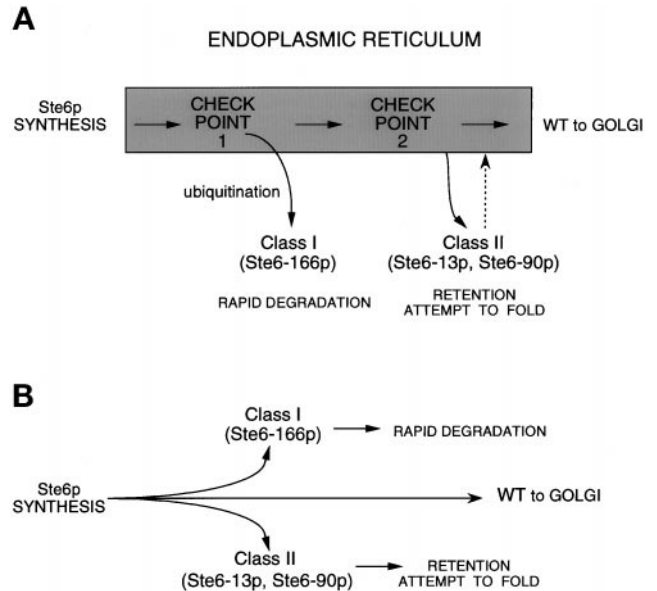


Figure 13. Models for ER quality control in yeast. (A) ER quality control is depicted as a linear pathway containing at least two "checkpoints." The first checkpoint is proposed to recognize poorly folded proteins (e.g., Ste6-166p) leading to their ubiquitination and rapid degradation by the proteasome. Proteins that proceed past the first checkpoint (i.e., Ste6-13p and Ste6-90p), yet are still misfolded, may be detained at a second checkpoint. This latter block could also lead to retention in the ER, giving misfolded proteins more time to fold correctly. Clearing the two steps proposed above might be a prerequisite for the exit of wild-type Ste6p from the ER or may influence mutant forms of Ste6p only. (B) ER quality control is shown as a nonlinear branched pathway in which the wild-type and mutant forms of Ste6p are channeled to distinct fates.

ically stable products and thus are in Class II. Instead, the fate of mutant forms of Ste6p is presumably determined by subtle differences in folding that direct it to distinct machinery.

A Linear Pathway for ER Quality Control in Yeast

Our finding that Ste6p can be channeled to different outcomes suggests a model for a linear pathway of ER quality control (Figure 13A). We postulate two distinct checkpoints at which folding could be monitored, based on the distinct phenotypes of Class I and Class II mutants. At the first checkpoint, a severely misfolded membrane protein such as Ste6-166p could be assessed as unfoldable and channeled for ubiquitination and rapid degradation. Less severely misfolded proteins (represented by Class II alleles) may pass surveillance at the first checkpoint and be remonitored at a second checkpoint, where there is the option to allow for possible refolding over a longer period of time. Our proposal for the particular order of the two steps in this linear pathway of ER quality control is supported by two observations. First, in situations

where Ste6-166p is not efficiently degraded, as is the case in mutants defective in the ubiquitin-proteasome degradation pathway, the usually rapidly degraded protein is stabilized and behaves as a phenocopy of Ste6-13p or Ste6-90p. This suggests that Ste6-166p can eventually be channeled into what seems to be the outcome reserved for Ste6-13p and Ste6-90p, and that ER accumulation occurs downstream of the events leading to proteasomal degradation. Second, the fact that the double mutant, Ste6-90,166p, is phenotypically indistinguishable from Ste6-166p in terms of its rapid degradation suggests that the checkpoint for Ste6-166p precedes the checkpoint that acts on Ste6-13p and Ste6-90p. The different ubiquitination pattern seen for Ste6-166p and Ste6-13p indicates that an early response in the first step of the pathway leads to ubiquitination of the protein, an event that does not appear to occur on mutant proteins that clear the first checkpoint. Thus, we speculate that exit from the first checkpoint, and therefore escape from ubiquitination, could still result in retention of the protein at the second checkpoint, possibly to allow the mutant protein to attempt to bind factors that promote a proper folded conformation or otherwise assist in exit from the ER.

An alternative model to explain the phenotypic difference between Class I and Class II mutants is shown in Figure 13B. According to this view, the mutant Ste6p proteins are channeled into separate and parallel fates, reflecting divergent responses by the ER quality control system. Quality control could therefore involve two different sets of machinery, one for rapid degradation and one for stable retention, that would independently recognize different kinds of folding defects. This latter view suggests a branched and not a linear pathway. Ultimately, it will be the identification and characterization of ER quality control components that allow us to distinguish unambiguously between these possibilities.

HRD2, an Allele-specific High-Copy Suppressor of Two ste6 Trafficking Mutants

The phenomenon of ER quality control was discovered a number of years ago, but the identification of components involved in the recognition and possible refolding of abnormal proteins has proceeded slowly. Using the integrated *ste6-90* mutation as a starting point, we identified the gene *HRD2* as a multicopy suppressor of the mating defect associated with this mutation (Figure 12). The *HRD2* gene was previously identified as required for the physiological degradation of the enzyme HMG-CoA reductase in the ER, since in a *hrd2* mutant, HMG-CoA reductase fails to undergo regulated degradation (Hampton *et al.*, 1996). *HRD2* shows significant homology to human p97, a component of the 19S proteasome cap (Tsurumi *et al.*,

1996), thereby implicating the proteasome in this degradative process.

Interestingly, the multicopy suppression of *ste6* mutants by *HRD2* is allele specific, in that 2μ *HRD2* suppresses the mating defect of *ste6-90* and *ste6-166*, but fails to suppress that of the other trafficking mutant, *ste6-13*, or of *ste6* mutants that are defective in function but not trafficking. The allele-specific suppression exhibited by 2μ *HRD2* for *ste6-90* and *ste6-166*, both of which are mutations that cause ER retention and that lie very close on the Ste6p molecule, is suggestive of a direct interaction between Hrd2p and these mutant Ste6p proteins.

The explanation for the mating suppression of *ste6-90* and *ste6-166* by overexpression of the proteasome subunit Hrd2p is not clear at present. The simplest possibility is that 2μ *HRD2* may improve the exit of the mutant Ste6p proteins from the ER. Although we did not detect an alteration in their half-life or localization, this could be due to the fact that a modest alteration in these parameters is challenging to detect, in contrast to improved mating, for which we have a very sensitive test. Alternatively, it is simply improved folding of these proteins that enhances their activity, suggesting a role for Hrd2p as a chaperone. The possibility that the proteasome could be involved in promoting the folding of certain molecules targeted for ERAD suggests a novel role for this cellular structure. Furthermore, the finding that there is an intersection between the process of ER quality control of aberrant proteins and the regulated ER degradation of wild-type HMG-CoA reductase provides a provocative hypothesis for further investigation.

ACKNOWLEDGMENTS

We thank C. Machamer for helpful comments on the manuscript; M. Hochstrasser and D. Wolf for strains and plasmids; M. Rose and E. Jones for antibodies and strains; D. Murphy and W. Guggino for generous help with microscopes and computers; and M. Bogyo and H. Ploegh for proteasome inhibitors. We thank members of the Michaelis laboratory for valuable ideas and G. Phan for technical assistance. This work was supported by National Institutes of Health grants GM-51508 and DK-48977 to S.M. and a fellowship (GM-18641) from the National Institutes of Health to W.K.S.

REFERENCES

- Amara, J.F., Cheng, S.H., and Smith, A.E. (1992). Intracellular protein trafficking defects in human disease. *Trends Cell Biol.* 2, 145-149.
- Berkower, C. (1995). Analysis of *STE6*, a *Saccharomyces cerevisiae* ATP Binding Cassette (ABC) Protein. Ph.D. Thesis. Baltimore, MD: Johns Hopkins University.
- Berkower, C., Loayza, D., and Michaelis, S. (1994). Metabolic instability and constitutive endocytosis of *STE6*, the *a*-factor transporter of *Saccharomyces cerevisiae*. *Mol. Biol. Cell* 5, 1185-1198.
- Berkower, C., and Michaelis, S. (1991). Mutational analysis of the yeast *a*-factor transporter *STE6*, a member of the ATP binding cassette (ABC) protein superfamily. *EMBO J.* 10, 3777-3785.

- Berkower, C., and Michaelis, S. (1996). ATP binding cassette proteins in yeast. In: *Membrane Protein Transport*, ed. S. Rothman, Greenwich, CT: JAI Press, 231–277.
- Biederer, T., Volkwein, C., and Sommer, T. (1996). Degradation of subunits of the Sec61p complex, an integral component of the ER membrane, by the ubiquitin-proteasome pathway. *EMBO J.* *15*, 2069–2076.
- Bogyo, M., McMaster, J.S., Gaczynska, M., Tortorella, D., Goldberg, A.L., and Ploegh, H. (1997). Covalent modification of the active site threonine of proteasomal B subunits and the *Escherichia coli* homolog HslIV by a new class of inhibitors. *Proc. Natl. Acad. Sci. USA* *94*, 6629–6634.
- Bonifacino, J.S., and Lippincott-Schwartz, J. (1991). Degradation of proteins within the endoplasmic reticulum. *Curr. Opin. Cell Biol.* *3*, 592–600.
- Brodsky, J.L., and McCracken, A.A. (1997). ER-associated and proteasome-mediated protein degradation: how two topologically restricted events came together. *Trends Cell Biol.* *7*, 151–156.
- Chen, P., Johnson, P., Sommer, T., Jentsch, S., and Hochstrasser, M. (1993). Multiple ubiquitin-conjugating enzymes participate in the in vivo degradation of the yeast Mata2 repressor. *Cell* *74*, 357–369.
- Doms, R.W., Keller, D.S., Helenius, A., and Balch, W.E. (1987). Role for adenosine triphosphate in regulating the assembly and transport of vesicular stomatitis virus G protein trimers. *J. Cell Biol.* *105*, 1957–1969.
- Elble, R. (1992). A simple and efficient procedure for transformation of yeasts. *Biotechniques* *13*, 18–20.
- Gaber, R.F., Copple, D.M., Kennedy, B.K., Vidal, M., and Mard, M. (1989). The yeast gene *ERG6* is required for normal membrane function but is not essential for biosynthesis of the cell-cycle-sparking sterol. *Mol. Cell. Biol.* *9*, 3447–3456.
- Geller, D., Taglicht, D., Edgar, R., Tam, A., Pines, O., Michaelis, S., and Bibi, E. (1996). Comparative topology studies in *Saccharomyces cerevisiae* and in *Escherichia coli* of the N-terminal half of the yeast ABC protein, Ste6. *J. Biol. Chem.* *271*, 13746–13753.
- Graham, T.R., Scott, P.A., and Emr, S.D. (1993). Brefeldin A reversibly blocks early but not late protein transport steps in the yeast secretory pathway. *EMBO J.* *12*, 869–877.
- Hammond, C., and Helenius, A. (1995). Quality control in the secretory pathway. *Curr. Opin. Cell Biol.* *7*, 523–529.
- Hampton, R.Y., Gardner, R.G., and Rine, J. (1996). Role of 26S proteasome and HRD genes in the degradation of 3-hydroxy-3-methylglutaryl-CoA reductase, an integral endoplasmic reticulum membrane protein. *Mol. Biol. Cell* *7*, 2029–2044.
- Heinemeyer, W., Gruhler, A., Mohrle, V., Mahe, Y., and Wolf, D.H. (1993). PRE2, highly homologous to the human major histocompatibility complex-linked RING10 gene, codes for a yeast proteasome subunit necessary for chymotryptic activity and degradation of ubiquitinated proteins. *J. Biol. Chem.* *268*, 5115–5120.
- Heinemeyer, W., Kleinschmidt, J.A., Saidowsky, J., Escher, C., and Wolf, D.H. (1991). Proteinase yscE, the yeast proteasome/multicatalytic-multifunctional proteinase: mutants unravel its function in stress induced proteolysis and uncover its necessity for cell survival. *EMBO J.* *10*, 555–562.
- Hiller, M.M., Finger, A., Schweiger, M., and Wolf, D.H. (1996). ER degradation of a misfolded luminal protein by the cytosolic ubiquitin-proteasome pathway. *Science* *273*, 1725–1728.
- Hochstrasser, M., Ellison, M.J., Chau, V., and Varshavsky, A. (1991). The short-lived MAT α 2 transcriptional regulator is ubiquitinated in vivo. *Proc. Natl. Acad. Sci. USA* *88*, 4606–4610.
- Hughes, E.A., Hammond, C., and Cresswell, P. (1997). Misfolded major histocompatibility complex class I heavy chains are translocated into the cytoplasm and degraded by the proteasome. *Proc. Natl. Acad. Sci. USA* *94*, 1896–1901.
- Ito, H., Fukuda, Y., Murata, K., and Kimura, A. (1983). Transformation of intact yeast cells treated with alkali cations. *J. Bacteriol.* *153*, 163–168.
- Jensen, T.J., Loo, M.A., Pind, S., Williams, D.B., Goldberg, A.L., and Riordan, J.R. (1995). Multiple proteolytic systems, including the proteasome, contribute to CFTR processing. *Cell* *83*, 129–135.
- Kaiser, C., Michaelis, S., and Mitchell, A. (1994). *Methods in Yeast Genetics: A Cold Spring Harbor Course Manual*, Cold Spring Harbor, NY: Cold Spring Harbor Laboratory Press.
- Kölling, R., and Hollenberg, C.P. (1994). The ABC-transporter Ste6 accumulates in the plasma membrane in a ubiquitinated form in endocytosis mutants. *EMBO J.* *13*, 3261–3271.
- Kölling, R., and Losko, S. (1997). The linker region of the ABC transporter Ste6 mediates ubiquitination and fast turnover of the protein. *EMBO J.* *16*, 2251–2261.
- Kopito, R.R. (1997). ER quality control: the cytoplasmic connection. *Cell* *88*, 427–430.
- Kuchler, K., Sterne, R.E., and Thorner, J. (1989). *Saccharomyces cerevisiae* STE6 gene product: a novel pathway for protein export in eukaryotic cells. *EMBO J.* *8*, 3973–3984.
- Lee, D.H., and Goldberg, A.L. (1996). Selective inhibitors of the proteasome-dependent and vacuolar pathways of protein degradation in *Saccharomyces cerevisiae*. *J. Biol. Chem.* *271*, 27280–27284.
- Loayza, D., and Michaelis, S. (1998). Role for the ubiquitin-proteasome system in the vacuolar degradation of Ste6p, the a-factor transporter in *Saccharomyces cerevisiae*. *Mol. Cell. Biol.* *18*, 779–789.
- McCracken, A.A., and Brodsky, J.L. (1996). Assembly of ER-associated protein degradation in vitro: dependence on cytosol, calnexin, and ATP. *J. Cell Biol.* *132*, 291–298.
- Michaelis, S., and Herskowitz, I. (1988). The a-factor pheromone of *Saccharomyces cerevisiae* is essential for mating. *Mol. Cell. Biol.* *8*, 1309–1318.
- Novick, P., Ferro, S., and Schekman, R. (1981). Order of events in the yeast secretory pathway. *Cell* *25*, 461–9.
- Paddon, C., Loayza, D., Vangelista, L., Solari, R., and Michaelis, S. (1996). Analysis of the localization of STE6/CFTR chimeras in a *Saccharomyces cerevisiae* model for the cystic fibrosis defect CFTR Δ F508. *Mol. Microbiol.* *19*, 1007–1017.
- Papa, F.R., and Hochstrasser, M. (1993). The yeast *DOA4* gene encodes a deubiquitinating enzyme related to a product of the human *tre-2* oncogene. *Nature* *366*, 313–319.
- Pilon, M., Schekman, R., and Romisch, K. (1997). Sec61p mediates export of a misfolded secretory protein from the endoplasmic reticulum to the cytosol for degradation. *EMBO J.* *16*, 4540–4548.
- Pind, S., Riordan, J.R., and Williams, D.B. (1994). Participation of the endoplasmic reticulum chaperone calnexin (p88, IP90) in the biogenesis of the cystic fibrosis transmembrane conductance regulator. *J. Biol. Chem.* *269*, 12784–12788.
- Plempner, R.K., Bohmler, S., Bordallo, J., Sommer, T., and Wolf, D.H. (1997). Mutant analysis links the translocon and BiP to retrograde protein transport for ER degradation. *Nature* *388*, 891–895.
- Romano, J.D., Schmidt, W.K., and Michaelis, S. (1998). The CAAX methyltransferase Ste14p is localized to the ER. *Mol. Biol. Cell* *9*, 2231–2247.
- Sikorski, R.S., and Boeke, J.D. (1991). In vitro mutagenesis and plasmid shuffling: from cloned gene to mutant yeast. In: *Methods in Enzymology: Guide to Yeast Genetics and Molecular Biology*, ed. C. Guthrie and G.R. Fink, San Diego CA: Academic Press, 302–318.

- Sikorski, R.S., and Hieter, P. (1989). A system of shuttle vectors and yeast host strains designed for efficient manipulation of DNA in *Saccharomyces cerevisiae*. *Genetics* 122, 19–27.
- Sommer, T., and Jentsch, S. (1993). A protein translocation defect linked to ubiquitin conjugation at the endoplasmic reticulum. *Nature* 365, 176–179.
- Taglicht, D., and Michaelis, S. (1998). A complete catalogue of *Saccharomyces cerevisiae* ABC proteins and their relevance to human health and disease. In: *Methods in Enzymology. ABC Transporters: Biochemical, Cellular, and Molecular Aspects*, ed. S.V. Ambudkar and M.M. Gottesman, New York: Academic Press.
- Thomas, P.J., Bao-He, Q., and Pedersen, P. (1995). Defective protein folding as a basis of human disease. *Trends Biochem. Sci.* 20, 456–459.
- Tsurumi, C., Shimizu, Y., Saeki, M., Kato, S., and Tanaka, K. (1996). cDNA cloning and functional analysis of the p97 subunit of the 26S proteasome, a polypeptide identical to the type-1 tumor-necrosis-factor-receptor-associated protein-2/55. *Eur. J. Biochem.* 239, 912–921.
- Ward, C.L., Omura, S., and Kopito, R.R. (1995). Degradation of CFTR by the ubiquitin-proteasome pathway. *Cell* 83, 121–127.
- Werner, E.D., Brodsky, J.L., and McCracken, A.A. (1996). Proteasome-dependent endoplasmic reticulum-associated protein degradation: an unconventional route to a familiar fate. *Proc. Natl. Acad. Sci. USA* 93, 13797–13801.
- Wiertz, E.J., Jones, T.R., Sun, L., Bogyo, M., Geuze, H.J., and Ploegh, H.L. (1996). The human cytomegalovirus US11 gene product dislocates MHC class I heavy chains from the endoplasmic reticulum to the cytosol. *Cell* 84, 769–779.
- Wiertz, E.J., Tortorella, D., Bogyo, M., Yu, J., Mothes, W., Jones, T.R., Rapoport, T.A., and Ploegh, H.L. (1996). Sec61-mediated transfer of a membrane protein from the endoplasmic reticulum to the proteasome for destruction. *Nature* 384, 432–438.